Journal of Computer-Aided Molecular Design, 9 (1995) 425–438
ESCOM

J-CAMD 304

Conformational behaviour of the antineoplastic peptide dolastatin-10 and of two mutated derivatives

Piercarlo Fantucci[a], Tiziana Marino[b], Nino Russo[b] and Anna Maria Villa[c,*]

[a]*Dip. di Chimica Inorganica, Università di Milano, Centro CNR, via Venezian 21, I-20133 Milan, Italy*
[b]*Dip. di Chimica, Università della Calabria, I-87036 Arcavacata di Rende, Cosenza, Italy*
[c]*Ist. di Chimica Farmaceutica e Tossicologica, Università di Milano, viale Abruzzi 42, I-20131 Milan, Italy*

Received 6 June 1995
Accepted 4 July 1995

Keywords: Cytostatic compounds; Tubulin; Mitosis inhibitors; Quenching; Ab initio optimization; Unusual amino acids; Conformational search

Summary

The three-dimensional structure of dolastatin-10, an extremely potent cytostatic and antineoplastic peptide extracted from the mollusc *Dolabella auricularia*, has not yet been fully characterized in an experimental way. By means of a systematic conformational search of the natural peptide and of two mutated analogs, carried out both in vacuo and in aqueous solution, the present work allows to obtain insights into the conformational preferences of this remarkable compound. In addition, the ability to form intra- and intermolecular H-bonds as a function both of the sequence and of the conformation is discussed. The search for the best molecular conformations has been carried out using a molecular mechanics approach, based on the CVFF potential. Dolastatin-10 contains some unusual amino acids for which no experimental structural data are available. In order to check the reliability of the CVFF potential in predicting structures of such nonconventional amino acids, geometry optimizations have been carried out using the ab initio Hartree–Fock procedure. The CVFF parameterization is found to be adequate also for nonconventional amino acids.

Introduction

The powerful properties of the Indian Ocean sea hare *Dolabella auricularia* were known already in the Roman age [1], where extracts of this opistobranch mollusc were employed for therapeutic or nefarious purposes because of their high toxicity.

More recently, Pettit and co-workers [2–12] devoted an extended study to the isolation and structural characterization of a large number of active principles contained in this remarkable marine animal. Among them one can find terpenes (e.g., dolatriol [2] and loliolide [3]), proteins (the cytolytic dolabellanins, see for instance Ref. 13) and a series of 15 low-molecular-weight depsipeptides and peptides called dolastatins [5].

Many of these compounds show cytotoxic activity, and they are thought to be an essential part of the chemodefensive devices of the soft-bodied and slowly moving sea hares. However, the most extraordinary properties are shown by the dolastatins, and particularly dolastatin-10 (compound **1**, see Scheme 1) and, to a slightly smaller extent, dolastatin-15. Indeed, due to the promising results of preliminary bioassays [5,6], which indicated the only two linear dolabella peptides to be among the most potent cytostatic and/or antineoplastic agents known to date, the isolation and structural characterization of the latter compounds were pursued during several years. This proved to be a particularly challenging task, due to their structural complexity (e.g., the presence of several chiral centres), the impossibility to obtain crystals and the extremely small quantities of active principles contained in molluscs.

Finally, it was found [5] that compound **1** is a pentapeptide with the structural formula reported in Scheme 1. The first residue is a dimethylated valine, called dolavaline (Dov). The second residue is a valine, while the third has been called dolaisoleuine (Dil). An N- and O-demethylated optical isomer of this amino acid is called statin

*To whom correspondence should be addressed.

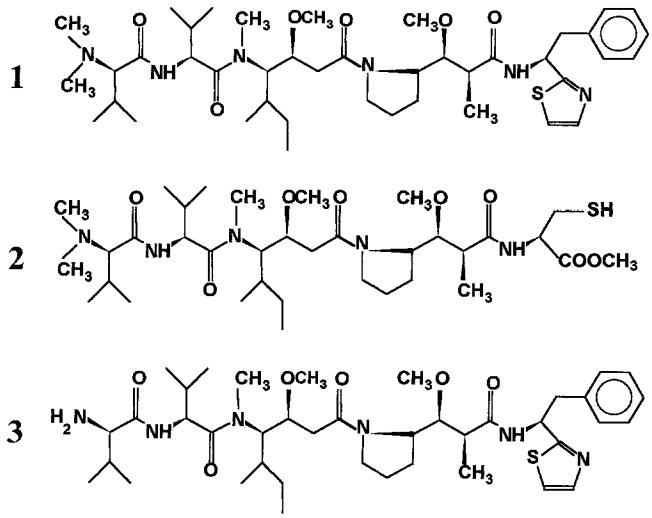

Scheme 1. Sequences of dolastatin-10 and two analogs. **1**: Dov-Val-Dil-Dap-Doe; **2**: Dov-Val-Dil-Dap-Cys-OMe; and **3**: Val^1-Val^2-Dil-Dap-Doe. Abbreviations for unusual amino acids: Dov = dolavaline; Dil = dolaisoleuine; Dap = dolaproine; Doe = dolaphenine.

[14] and it is a component of a well-known inhibitor of acid proteases (like pepsin, renin and cathepsin) called pepstatin; the next amino acid, called dolaproine (Dap), is a γ-amino acid characterized by the presence of a pyrrolidine ring enclosing the nitrogen involved in the peptide bond. The last residue (dolaphenine (Doe)) contains a thiazole moiety, which, although rather rare in natural compounds, is present in another dolabella active principle, dolastatin-3 [4]. To the same backbone carbon which carries the thiazole ring, a benzyl moiety is bound. The result is a bulky, rather electron-rich system without any carboxylic function, which can be hypothesized to affect both the conformation and the reactivity of the molecule towards the biological partner.

The total synthesis of **1**, which was accomplished in 1988 by Pettit et al. [7], allowed to plan a large-scale assay against NCI human cancer cell lines, human xenografts and murine cancer systems [4], confirming the extremely high potency of the peptide. Compound **1** proved to be one of the most potent known agents against several types of cancer, and is planned to enter phase I clinical trials.

With regard to the action mechanism, different types of activity have been observed for **1**. Besides its pronounced cytotoxicity, **1** has been shown to be a potent inhibitor of tubulin polymerization [10–12] and a non-competitive inhibitor of the binding of vinca alkaloids to tubulin. In addition, inhibition of binding of GTP to tubulin, but no displacement of the nucleotide by **1** has been observed. This allowed the development of a schematic model for the possible interaction of dolastatin-10 and other peptide drugs with the β-unit of tubulin, which includes the presence of a peptide binding site, a 'vinca region' and an exchangeable GTP site.

An X-ray diffraction analysis was only possible on one of the several optical isomers of **1**, namely (6*R*)-isodolastatin-10 [8]; besides this, the only source of information about the three-dimensional structure of **1** are two-dimensional NMR studies, which confirmed the basic structural features and the amino acid sequence [5].

On the other hand, the presence of uncommon amino acids and residues makes it rather difficult to predict a 3D structure of **1** by computer modelling. One of the aims of the present study is, therefore, to present the results of a molecular mechanics (MM) and molecular dynamics (MD) simulation of the natural compound, **1**. In addition, in order to explore the possible influence of the terminal residues on the overall conformation and interaction capabilities of the peptide, the same study was carried out on compounds **2** and **3** (see Scheme 1). These were generated by the replacement of the C- and/or N-terminal residue of **1** with common amino acids. In particular, compound **2**, in which dolaphenine was replaced with the common amino acid cysteine, has been investigated in order to clarify the role and importance of the non-amino acidic residue, which, besides its apparent responsibility for the vinca-alkaloid antagonism of dolastatin-10 [10], was supposed to affect the 3D structural properties of **1**.

The analysis of the conformational features of the mutated peptides may help to define and monitor important properties (e.g., the tendency to form intra- and intermolecular H-bonds), which depend both on the sequence and the 3D structure, and which may dramatically affect the interaction potentialities. In fact, the replacement of dolavaline with valine (as in compound **3**), while increasing the hydrophilicity of the system, introduces an additional candidate hydrogen-bond donor (the primary amino group).

This information, taken together, may provide a better insight into the structural characteristics that are required for the natural peptides to interact with the biochemical events involved in tubuline polymerization and the mitotic process.

Computational methods

Molecular mechanics and molecular dynamics calculations have been carried out using the INSIGHT and DISCOVER programs of Biosym [15], based on the CVFF potential. As is well known, CVFF does not include parameters specific for a given amino acid, but, on the contrary, it is based on the characteristics of a given atom and its chemical surroundings.

To our knowledge, CVFF has never been applied to structural studies concerning nonconventional amino acids like those considered in the present study. In addition, a complete set of structural data for the amino acids Dov, Dap, Dil and Doe is still lacking. In order to obtain

such extremely important information, which is also useful to check the CVFF parameterization, a geometry optimization of the amino acids described above has been carried out using an ab initio Hartree–Fock (HF) method, and two different basis sets, namely STO-3G (basis A [16]) and 4-31G (basis B [16]). The best HF geometry structures of the amino acids Dov, Dil, Dap and Doe are compared with those obtained by the MM optimization with the standard CVFF parameterization (see below).

The sampling of the conformational space has been carried out along MD trajectories produced from different initial conditions. In order to minimize the computational costs, the simplest version of the CVFF, including the diagonal elements only, has been adopted.

The initial 3D structures of the systems investigated (**1**–**3**) have been generated using the geometries of the separated constituent amino acids obtained by CVFF optimization. As will be shown, such structures are fairly close to those obtained at an ab initio level. The guessed structures of **1**–**3** have been subjected to a first geometry optimization, leading to the starting conformation for the subsequent MD runs. The MD simulations have been carried out both in vacuo and in water, at constant energy (NVE ensemble), with a time step of 1 fs for a total period of 100 ps.

It is important to observe that, when MD calculations are carried out, the length of the time interval during which the system is supposed to reach nearly equilibrated conditions is of minor importance if the main goal is just sampling the conformational space. In our case, however, the initial part of each trajectory was considered as the equilibration period, and therefore was not included in the subsequent quenching operations, in order to avoid very improbable structures. In order to have a broader sampling of the conformational space, the following procedure was adopted, both in vacuo and in water solution.

A first MD (NVE) run was started by depositing the molecule at a total kinetic energy corresponding to a temperature of 300 K. Sampling of the second half of the trajectory every 5 ps allowed the extraction of 11 frames, which were subjected to a geometry optimization. From these 11 conformers, the lowest energy conformer was used as the starting point for a second MD (NVE) simulation, with an initial kinetic energy corresponding to 400 K. After quenching also the frames extracted from the second half of the new trajectory, the lowest energy conformer (if different from that already located) was used again as a seed conformation for a third MD run. The reference temperature at the start of this run was equal to 500 K. A final quenching resulted in a new series of 11 conformers. Thus, a total sample of 33 conformers in vacuo and 33 conformers in water has been examined for each compound. This procedure may be considered as a sort of repeated process of heating–quenching, similar in aim to a simulated annealing experiment.

The procedure was applied to the study of the three peptides, both in vacuo and in solution and both in the base and in the protonated form (see below), and allowed location of a few well-defined minima, which can be quite reliably considered to be the lowest energy conformers in the isolated phase, and a slightly higher number of low-energy forms in the condensed phase.

All molecules were considered both in a neutral form and in the form protonated at the Dov nitrogen for **1** and **2**, and at the Val[1] nitrogen for compound **3**. Deprotonation of the cysteine carboxylic moiety in **2** was excluded by 'capping' it through methyl esterification. The protonated forms are called **1h**, **2h** and **3h**.

For the solvated systems **1**–**3**, the first MD simulations were carried out starting from the corresponding best conformer obtained in vacuo in the presence of about 190 water molecules, constrained in a sphere with a radius of 12 Å. The distribution of water molecules, initially generated in a random manner, was subjected to a preliminary optimization before starting the dynamics calculations.

The number of water molecules is probably insufficient to represent the very detailed nature (in particular the energetics) of the hydration process, but it was found to be sufficient to illustrate the occurrence of the water–solute H-bonds, including all the atoms which are expected to act as acceptor or donor sites on the basis of their net charge. The largely prevailing acceptor character of the molecules is evidently due to the nature of their sequences, which contain a rather high number of carbonyl groups and several tertiary, but few secondary nitrogens (only one primary amine function is present in the Val[1] residue of **3**), almost all engaged in amidic groups.

In the case of the protonated species **1h**–**3h** (in vacuo and in the presence of about 190 water molecules), only a unique trajectory was run, thus avoiding the very time-consuming iterative procedure described above. However,

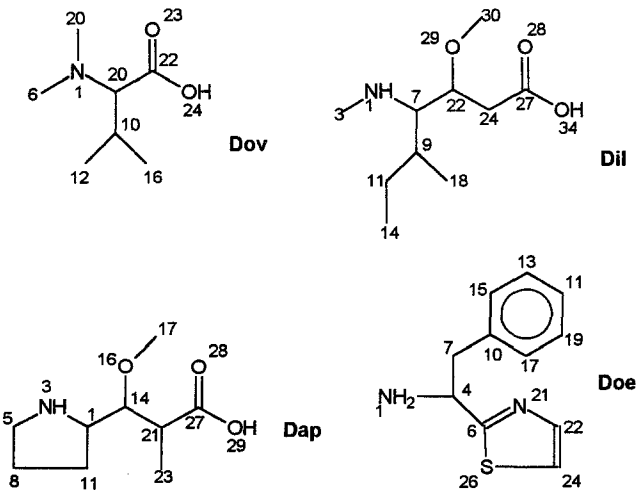

Scheme 2. Unusual amino acids in dolastatin-10 with the numbering of their 'heavy' atoms adopted in the ab initio study.

TABLE 1
COMPARISON BETWEEN THE GEOMETRIES OF THE UNUSUAL AMINO ACIDS IN DOLASTATIN-10 (FORMULAS AND ATOM NUMBERING IN SCHEME 2) FROM AB INITIO AND CVFF OPTIMIZATION

Atoms	Bond distance (Å)			Atoms	Valence angle (°)			Atoms	Torsion angle (°)		
	CVFF	STO-3G	4-31G		CVFF	STO-3G	4-31G		CVFF	STO-3G	4-31G
Dov											
1-2	1.49	1.48	1.46	1-20-10	114.3	117.3	116.0	2-1-20-22	64.0	105.2	95.3
1-6	1.49	1.48	1.46	2-1-20	117.9	118.2	122.2	6-1-20-10	153.9	111.6	120.2
1-20	1.52	1.50	1.46	10-20-22	113.4	112.6	112.5	6-1-20-22	76.0	121.7	111.7
10-12	1.55	1.55	1.54	12-10-20	114.3	111.6	110.1	12-10-20-1	60.3	66.4	62.1
10-16	1.55	1.55	1.54	16-10-20	113.9	111.4	112.9	1-20-22-23	98.0	166.8	160.0
10-20	1.58	1.57	1.56	20-22-23	123.8	124.3	123.3	1-20-22-24	82.0	11.3	19.7
20-22	1.56	1.58	1.53	20-22-24	112.3	114.4	115.8				
22-23	1.23	1.22	1.20								
22-24	1.37	1.38	1.34								
Dil											
1-3	1.49	1.48	1.46	1-7-9	117.5	118.8	116.5	3-1-7-22	85.6	88.6	86.2
1-7	1.51	1.49	1.46	1-7-22	111.5	109.3	110.2	1-7-9-11	75.1	71.1	69.8
7-9	1.58	1.57	1.55	3-1-7	119.0	118.2	123.6	1-7-9-18	54.6	57.0	57.4
7-22	1.58	1.57	1.54	7-9-11	116.8	116.1	116.2	1-7-22-24	166.5	167.8	171.7
9-11	1.56	1.55	1.54	7-9-18	112.4	109.8	109.1	7-9-11-14	157.3	159.3	159.9
9-18	1.55	1.55	1.54	7-22-24	113.6	111.4	112.9	7-22-24-27	171.3	173.2	174.9
11-14	1.54	1.54	1.53	7-22-29	112.9	115.3	113.6	7-22-29-30	112.6	106.0	107.7
22-24	1.55	1.55	1.54	9-11-14	115.0	112.6	113.0	22-24-27-28	120.8	120.8	120.7
24-27	1.52	1.55	1.51	22-24-27	115.7	111.6	113.7	22-24-27-34	60.3	60.3	60.9
27-28	1.23	1.22	1.20	22-29-30	116.5	111.7	117.6				
27-34	1.36	1.39	1.35	24-27-28	123.6	124.1	124.0				
29-30	1.45	1.44	1.44	24-27-34	111.9	114.8	115.1				
Dap											
1-3	1.48	1.50	1.47	1-11-8	103.8	105.8	102.3	11-1-3-5	30.7	31.0	33.6
1-11	1.53	1.55	1.53	1-14-16	108.5	107.6	108.2	3-1-11-8	39.4	39.0	38.6
3-5	1.48	1.50	1.48	1-14-21	114.0	111.2	112.0	1-3-5-8	9.7	10.7	14.6
5-8	1.53	1.56	1.56	3-1-11	110.6	105.4	104.1	3-1-14-16	170.9	175.2	170.5
8-11	1.53	1.54	1.54	11-1-14	113.9	111.6	111.3	3-5-8-11	15.9	13.6	10.0
14-16	1.46	1.44	1.42	3-5-8	105.0	107.8	106.2	5-8-11-1	34.8	31.4	29.3
14-21	1.57	1.57	1.55	5-8-11	104.2	104.3	104.7	1-14-16-17	129.6	131.6	131.6
16-17	1.44	1.43	1.44	14-16-17	117.2	111.7	119.3	1-14-21-23	73.1	78.5	77.2
21-23	1.55	1.54	1.53	14-21-23	114.4	112.5	113.2	14-21-27-29	90.4	88.8	85.7
21-27	1.55	1.56	1.51	14-21-27	110.9	109.9	108.6				
27-28	1.23	1.21	1.20	21-27-28	124.6	124.7	124.9				
27-29	1.37	1.40	1.36	21-27-29	111.9	116.6	115.9				
				23-21-27	112.5	109.8	110.5				
Doe											
1-4	1.48	1.49	1.46	1-4-7	107.7	107.3	108.6	1-4-6-21	124.2	90.8	89.0
4-6	1.53	1.54	1.51	4-6-21	125.1	120.5	124.0	1-4-7-10	170.0	168.3	171.4
4-7	1.55	1.56	1.54	4-6-26	119.0	123.7	122.8	4-6-21-22	176.5	175.7	172.3
6-21	1.34	1.30	1.27	4-7-10	116.8	115.0	116.2	4-7-10-17	82.6	75.6	76.2
6-26	1.83	1.75	1.71	6-21-22	112.4	109.1	109.1	7-10-17-19	179.6	178.1	178.6
7-10	1.54	1.53	1.51	7-10-15	113.6	120.9	112.9	13-11-19-17	0.0	0.1	0.1
10-15	1.40	1.39	1.39	10-15-13	112.9	120.8	113.6	11-13-15-10	0.2	0.1	0.3
11-17	1.40	1.39	1.39	10-17-19	120.3	120.7	120.9	10-17-19-11	0.0	0.0	0.0
11-13	1.39	1.38	1.38	11-13-15	120.0	120.1	120.2	21-22-24-26	0.0	0.1	0.1
11-19	1.39	1.39	1.38	11-19-17	120.0	120.1	120.2	22-24-26-6	0.4	0.0	0.0
13-15	1.39	1.38	1.38	13-11-19	120.1	119.6	119.4	26-6-21-22	0.7	0.3	0.1
17-19	1.39	1.38	1.38	22-24-26	110.2	111.2	110.3				
21-22	1.37	1.43	1.40								
22-24	1.37	1.33	1.33								
24-26	1.72	1.73	1.80								

in order to keep the sampling space as broad as possible, a time duration of the trajectory equal to 250 ps was adopted. The initial atomic velocities were generated, as in the previous case, by a random distribution of the kinetic energy, corresponding to a temperature of 500 K. Sampling of the last 50 ps of the trajectory every 5 ps allowed the extraction of 11 frames, which were subjected to a geometry optimization.

It is worth noting that the above reported values of the temperature are only indicative of the initial amount of kinetic energy deposited in the system. For all the NVE trajectories, the starting temperatures decreased within a very short period (1–5 ps) to values fluctuating around 200 K, independent of the initial value.

Results and Discussion

The ab initio determination of the structures of Dov, Dil, Dap and Doe

The molecular structures of the unusual amino acids dolavaline, dolaisoleuine, dolaproine and dolaphenine have been determined by geometry optimization, carried out at the HF level. The results are listed in Table 1 and the numbering of the atoms is reported in Scheme 2. The CH, NH and OH distances, not reported in Table 1 for brevity, have average values equal to 1.090 (Csp^3H), 1.080 (Csp^2H), 1.030 (NH) and 0.991 Å (OH) for basis A and 1.085 (Csp^3H), 1.070 (Csp^2H), 0.995 (NH) and 0.957 Å (OH) for basis B. The corresponding (average) values obtained from the MM calculations based on CVFF (in Å) are 1.11 (Csp^3H), 1.08 (Csp^2H), 1.03 (NH) and 0.96 (OH).

Again, for brevity, we do not comment in detail on all the values concerning the valence and dihedral angles involving the H atoms. The agreement between the results obtained with basis A and basis B is satisfactory, i.e., the predicted values are coincident within a range of about $\pm 3°$ for valence angles and $\pm 20°$ for dihedral angles. A similar agreement was found, in general, also for the values given by CVFF.

The agreement between the CVFF and the ab initio results concerning the backbone geometry of the amino acids reported in Table 1 can be considered as fairly satisfactory, at least to an extent that allows the routine use of the CVFF potential for studies on the dolastatin derivatives.

In general, the CVFF bond distances coincide with the ab initio values to within 0.02 Å. The only evident exceptions are the bond distances involving the C_6 atom of Doe (see Scheme 2), belonging to the thiazole ring.

A maximum discrepancy of 4–5° can be observed for valence angles computed ab initio and with the CVFF. Finally, considering the usual flexibility which characterizes torsion angles, one can observe that the agreement between ab initio and CVFF results is basically satisfactory. Again, a case not completely satisfactory was found for dolaphenine, where the torsion angle controlling the orientation of the thiazole ring with respect to the N_1-C_4-C_6 plane is equal to 124° in CVFF, and about 90° in the geometry predicted at the ab initio level.

As far as the torsional angles are concerned, another difference is observed for the disposition of the dolavaline carboxyl oxygens. Indeed, the ab initio calculation predicts substantial coplanarity between the plane of the carboxylate group and that defined by N_1-C_{20}-C_{22} (see Scheme 2). In contrast, the CVFF optimization affords a conformer where the carboxylate plane lies approximately at right angles with respect to the N_1-C_{20}-C_{22} plane. However, the rotation involved, that of the Dov C^{α}-C(O) bond, controls the conformations of the *N*-dimethylamino moiety and the isopropyl side chain only. Since dolavaline

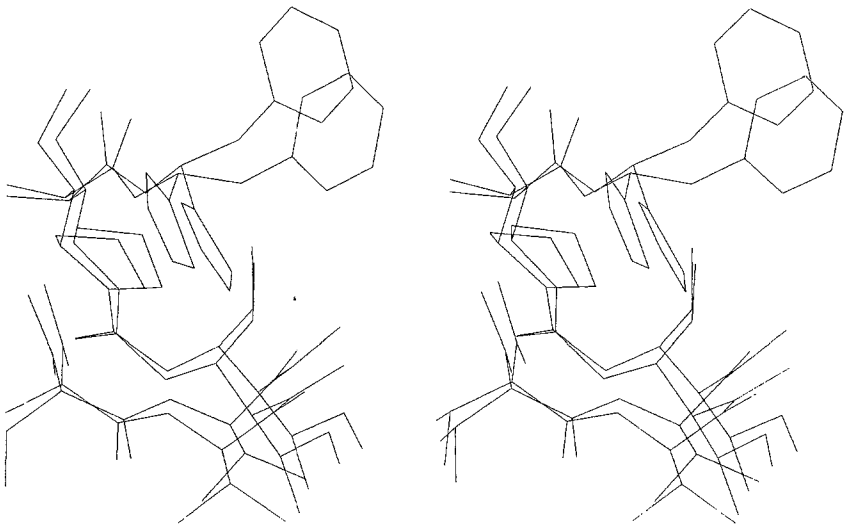

Fig. 1. Superposition of the two lowest energy conformers of compound **1** in vacuo. Hydrogens are omitted for clarity.

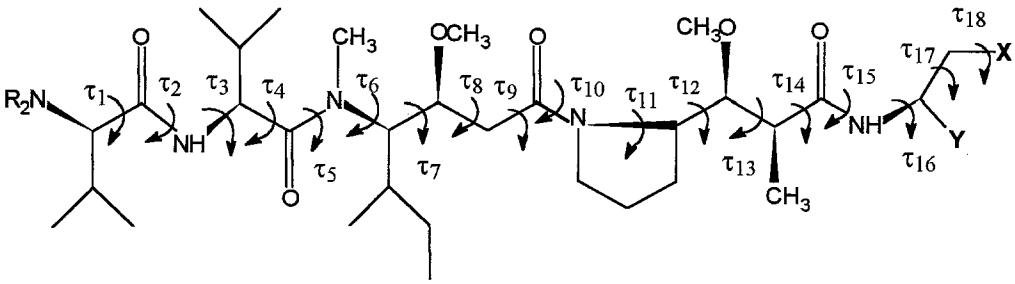

Fig. 2. Definition of the torsion angles in dolastatin-10 and its mutated analogs. X = C_6H_5, SH; Y = thiazole, $COOCH_3$; and R = H, CH_3 (see Scheme 1).

is the N-terminal amino acid, which should have more conformational freedom anyway, this difference in behaviour can probably be neglected in the case of the nonprotonated species.

When the Dov nitrogen is protonated, the conformation of the N-terminus could be of greater importance because of the orientation of possible intramolecular H-bonds formed by Dov-NH^+. However, the results described below and the frequent occurrence of such an H-bond seem to indicate that the overwhelming effect of the presence of the unitary charge largely prevails over the other potential components in determining the conformation of the N-terminal section.

Conformational properties

Dolastatin-10 (1)

The MD procedure described above, when applied to the isolated molecule **1**, allowed the identification of only two low-energy conformers. These are depicted in Fig. 1. In fact, almost all of the frames extracted from the three trajectories described above converge, after quenching, to a single minimum (A). This minimum is about 10 kcal mol^{-1} more stable than the one located in a previous study [17], which had a quasi-cyclic molecular shape. The definition of the torsion angles is illustrated in Fig. 2, and their values for the lowest energy conformers of the isolated compound **1** are listed in Table 2.

The conformer **1A** is rather folded and strongly S-shaped. This should be mainly due to hydrophobic effects, because no intramolecular H-bond is present. Another factor that favours the terminal N atom approaching the Doe portion is probably the electrostatic attraction between the Dov nitrogen, which is negatively charged, and the sulphur atom of Doe, with a positive net charge. In addition, the two cyclic substituents of Doe

TABLE 2
TORSIONAL GEOMETRIES OF THE LOWEST ENERGY CONFORMERS OF 1 AND **1h** IN VACUO AND IN WATER[a]

Torsion angle	$\mathbf{1}_v$**A**	$\mathbf{1}_v$**B**	$\mathbf{1}_w$**A**	$\mathbf{1}_w$**B**	$\mathbf{1}_w$**C**	$\mathbf{1h}_v$	$\mathbf{1h}_w$
τ_1	16.6	11.0	−80.0	−72.0	−72.5	−97.6	−44.1
τ_2	−176.2	−174.6	−179.5	−178.1	180.0	164.5	169.2
τ_3	−122.5	−122.4	−120.7	−120.6	−122.4	−93.9	−91.5
τ_4	89.8	85.4	87.8	95.3	90.2	129.3	123.8
τ_5	−12.6	−6.5	−5.3	−21.3	−10.7	6.9	15.9
τ_6	−105.5	102.4	−115.5	−110.3	−117.2	−87.2	−92.4
τ_7	160.1	167.5	149.5	145.4	142.1	171.3	174.7
τ_8	−150.9	−158.7	−176.3	−161.5	−163.5	−156.4	−156.6
τ_9	−86.7	−88.3	−154.6	−148.9	−148.2	−90.0	−88.3
τ_{10}	172.4	176.1	178.8	−171.2	−168.2	175.7	175.7
τ_{11}	−88.4	−88.5	−92.9	−90.9	−87.4	−88.9	−87.4
τ_{12}	80.0	80.0	79.0	73.8	80.6	71.8	74.6
τ_{13}	−140.1	−152.9	−157.3	−162.2	−170.9	−165.7	−163.8
τ_{14}	136.6	110.1	144.4	90.4	97.9	−73.0	−81.4
τ_{15}	176.4	175.0	−163.8	−165.4	−156.5	−178.6	−177.1
τ_{16}	86.8	86.3	104.8	130.9	136.8	126.4	147.7
τ_{17}	−175.1	−169.9	−61.8	−61.0	−58.1	−78.1	−71.7
τ_{18}	76.3	82.9	−67.7	−70.7	−70.9	−100.9	−93.8
ΔE	0	0.68	0	0.33	3.13		

[a] τ_i are torsion angles in degrees; see Fig. 2 for their definition. $\mathbf{1}_v$**A** and $\mathbf{1}_v$**B** represent the lowest energy conformers of **1** in vacuo; $\mathbf{1}_w$**A**, $\mathbf{1}_w$**B** and $\mathbf{1}_w$**C** are conformers of **1** in water, with increasing relative energy (ΔE, kcal mol^{-1}). $\mathbf{1h}_v$ and $\mathbf{1h}_w$ represent the lowest energy conformers of **1h** in vacuo and in water, respectively.

display a mutual attraction, which cannot give rise to a real π-π stacking, because the spacer chain between them is too short.

An interesting feature is the presence of a cis peptide bond between the valine and dolaisoleuine residues. The corresponding torsion angle assumes a value of about −12°. This behaviour is probably due to the simultaneous presence of a methylated amidic nitrogen, the bulky side chains of valine and dolaisoleuine and a methoxy group at the β-carbon of dolaisoleuine. All other peptide bonds in the molecule show a slight deviation from planarity (with oscillations of ±10° around the value 180°) due to the presence of bulky substituents which exert a mutual repulsion.

Conformer **1B** lies only 0.7 kcal mol^{-1} above the most stable form **1A**. The Dov-Dap parts of the two conformers show a substantial superimposability, whereas a noticeable difference in the backbone disposition is observed for the residue dolaisoleuine. This also affects the value of the angle corresponding to the cis peptide bond, about −7°. The major difference lies, however, in the disposition of the aromatic moieties of the dolaphenine residue (see Fig. 1 and torsion angle τ_{14} in Table 2).

In water, three low-energy conformers could be identified. The most stable minimum (conformer A, see Fig. 3 and Table 2) has been obtained by quenching the trajectory with an initial temperature of 400 K at a time step of 100 ps. An almost degenerate conformer (B) has been obtained by minimizing the structure at 65 ps of the trajectory starting at 500 K, and another (C), with an energy difference less than 3.5 kcal mol^{-1}, at 50 ps of the same trajectory. In Fig. 3 the superposition of the three conformers is shown. As can be seen, the global S-shape is retained. In fact, a substantial identity in conformation is observed for the three N-terminal residues. Major variations are associated with the geometry of Dov and Doe only, and in particular with the rings of the latter residue, which are interchangeable in spatial disposition without an appreciable energy loss.

Conformer B shows the largest deviation from planarity (−21°, see Table 2) of the cis peptide bond between valine and dolaisoleuine, whereas all three conformers show rather distorted peptide bonds between Dap and Doe, with values ranging from −165° to −156°.

None of the conformers have been found to form intramolecular hydrogen bonds.

*Dolastatin-10 – protonated species (**1h**)*

The quenching procedure on the last 50 ps dynamics of compound **1h** in vacuo produced one single minimum conformer, in which a cis peptide bond between the residues valine and dolaisoleuine and a slight deviation from planarity of all peptide bonds were observed. In contrast to the behaviour of the nonprotonated compound **1**, the corresponding ammonium compound does form two intramolecular hydrogen bonds, one between the Dap carbonyl oxygen and the Dov NH^+ proton, and the other between the Doe NH and the Dap OCH_3 oxygen. Indeed, when the torsional geometry of **1h** is compared with the minimum of the base (see Table 2), it is observed that the greater differences affect the angles τ_1, τ_3, τ_4 and τ_{14}, the values of which allow the two H-bonded moieties to approach each other. Torsion angle τ_2 retains its value of about 180°, representing the trans peptide bond between dolavaline and valine.

The last part of the trajectory of compound **1h** in the presence of water molecules afforded several minima, which, however, lie at a rather high energy level. The lowest energy conformer (depicted in Fig. 4) was located optimizing the structure at a time step of 240 ps, and has a CVFF energy of about 20 kcal mol^{-1} lower than the next minimum. It does not show any intramolecular H-

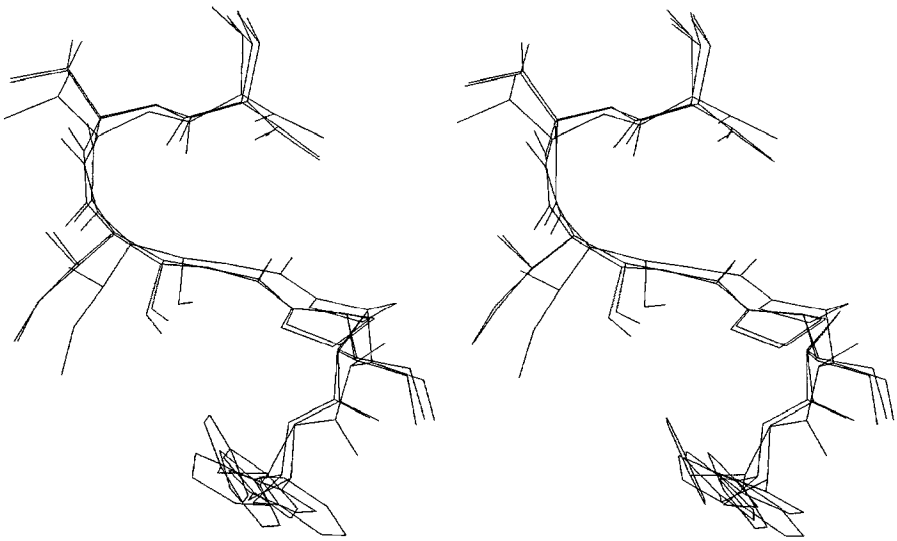

Fig. 3. Superposition of the three lowest energy conformers of compound **1** in water. Hydrogens and water molecules are omitted for clarity.

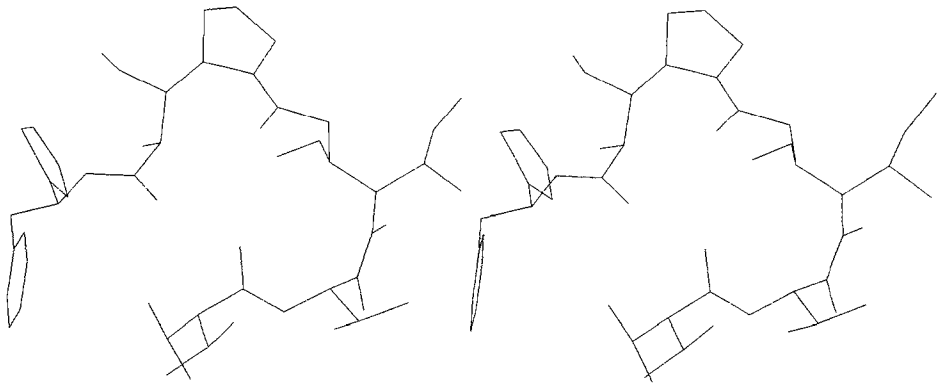

Fig. 4. Minimum-energy conformation of compound **1h** in water. Hydrogens and water molecules are omitted for clarity.

bond. The value of τ_1 (see Table 2), which exhibits the largest difference with respect to the base form, shows that the NH^+ proton is directed towards the solvent. The rest of the structure resembles that of the nonprotonated species. The cis bond between residues Val and Dil is still a bit more distorted ($\tau_5 \approx 17°$).

Nonnatural derivatives

The cysteine derivative of dolastatin-10 (2) In compound **2**, the dolaphenine of **1** is replaced by a cysteine residue (see Scheme 1) with an esterified carboxylic group.

The MD simulation described in the previous section, carried out in vacuo, allowed the location of five energy minima in a range of 2 kcal mol^{-1}. Three of them are almost degenerate, and they all have a quite similar geometry (see Table 3). Again, the portion of the molecule corresponding to the first three residues is virtually identical in all the identified conformers. The cis peptide bond is perfectly planar. This represents a quite important difference with the results found for **1**: it seems evident that the deviation from planarity present in **1** can be ascribed to the interactions between the bulky C-terminal group rings and the N terminus. The carboxylate group locates itself in the direction of the thiazole group of **1**, whereas the cysteine SH group points towards the region occupied by the benzyl moiety.

It is worth noting that in the case of compound **2**, the MD run started at 500 K in the presence of water resulted in the identification of high-energy conformers only. One conformer (depicted in Fig. 5; the torsional geometry is listed in Table 3) was found to be far more stable than the others (about 8 kcal mol^{-1} lower in energy

TABLE 3
TORSIONAL GEOMETRIES OF THE LOWEST ENERGY CONFORMERS OF **2** AND **2h** IN VACUO AND IN WATER[a]

Torsion angle	$\mathbf{2}_v$	$\mathbf{2}_w$	$\mathbf{2h}_v\mathbf{A}$	$\mathbf{2h}_v\mathbf{B}$	$\mathbf{2h}_w\mathbf{A}$	$\mathbf{2h}_w\mathbf{B}$
τ_1	6.6	−75.4	−111.2	−92.2	−104.8	−85.3
τ_2	−176.3	169.8	−179.2	−173.5	−173.5	178.9
τ_3	−119.4	−107.7	−109.8	−109.8	−125.5	−127.3
τ_4	86.0	92.0	99.0	97.1	99.0	98.8
τ_5	−1.8	10.8	−8.4	−6.4	−9.0	−13.6
τ_6	−104.0	−110.2	−98.7	−101.7	−100.8	−106.5
τ_7	168.9	164.6	168.5	165.1	162.8	167.8
τ_8	−158.3	−172.2	−164.0	−162.0	−155.6	−149.8
τ_9	−90.1	−99.1	−105.6	−110.2	−99.0	−120.7
τ_{11}	179.8	−173.6	179.0	−169.8	168.7	−173.6
τ_{11}	−89.1	−91.0	−73.3	−72.1	−78.0	−73.1
τ_{12}	73.3	71.0	143.2	151.4	146.9	146.4
τ_{13}	−158.6	−162.6	−151.5	−152.0	−166.1	−156.2
τ_{14}	97.5	69.0	−67.0	−61.1	−90.1	−89.0
τ_{15}	174.6	167.7	168.7	165.9	176.4	165.9
τ_{16}	−129.7	−129.7	147.0	139.8	144.4	110.7
τ_{17}	−57.8	−109.9	−83.6	−84.4	118.6	−71.3
ΔE			0	1.52	0	1.54

[a] τ_i are torsion angles in degrees; see Fig. 2 for their definition. $\mathbf{2}_v$ and $\mathbf{2}_w$ represent the lowest energy conformers of **2** in vacuo and in water, respectively. $\mathbf{2h}_v\mathbf{A}$ and $\mathbf{2h}_v\mathbf{B}$ are the lowest energy conformers of **2h** in vacuo, with increasing relative energy (ΔE, kcal mol^{-1}); $\mathbf{2h}_w\mathbf{A}$ and $\mathbf{2h}_w\mathbf{B}$ represent the lowest energy conformers of **2h** in water, also with increasing relative energy.

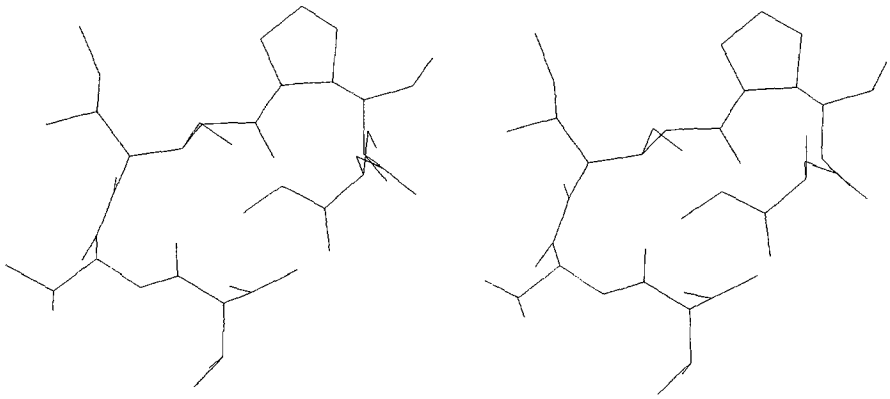

Fig. 5. Minimum-energy conformation of compound **2** in water. Hydrogens and water molecules are omitted for clarity.

with respect to the next one). This conformer was obtained by quenching the molecular structure of **2** at 70 ps in the trajectory starting at 400 K. If the somewhat less stable conformers are considered, one can observe a pronounced rigidity as far as the residues Dil and Dap are concerned, a slightly greater freedom for Dov, and a pronounced spatial variability, as expected, for the less bulky C-terminal residue cysteine.

The most stable conformer is S-shaped as well. However, the S-shape is far smoother compared to **1**, probably because of two opposite effects: the lack of attraction between the N-terminal nitrogen and the thiazole S (indeed, the electron-rich ester group is more likely repulsive towards the N-terminal) and the reduced volume of the substituents at the C-terminal portion, which reduces steric interaction.

In one case (the conformer obtained by quenching the structure at 100 ps of the trajectory started at 300 K), a hydrogen bond is observed between the dolavaline N and the valine NH.

*The protonated cysteine derivative of dolastatin-10 (**2h**)* Three low-energy conformers were located for the isolated compound **2h**. These were found as a result of quenching the points at 220, 225 and 245 ps for conformers A, B and C, respectively, although all other conformers obtained after 230 ps were found to be identical to either A or B. Their geometries are also quite similar: A and B differ only in the value of τ_1 by 20° and by a few degrees in all other torsion angles (see Table 3). These differences give as a global result a slightly changed disposition of the peripheral amino acids. In the case of conformer C, the only variation with respect to A is the extent of flipping of the dolaproine pyrrolidine ring.

All three conformers show two intramolecular H-bonds, one between an ammonium proton and the dolaproine CO and the other between the cysteine NH and the dolaproine OCH_3, a situation similar to that of the minimum of **1h**.

The quenching of the trajectory of **2h** in the presence of 190 water molecules gave two particularly low-energy conformers, with an energy difference of about 1.5 kcal mol^{-1}. These were derived from points at 210 (conformer A) and 225 ps (conformer B) and are shown in Fig. 6. Both exhibit an intramolecular H-bond between the ammonium proton and the dolaisoleuine carbonyl oxygen. The differences among the two conformers mainly involve the conformation of the peripheral amino acids (as expected), but the value of τ_9, in the core of the peptide, is quite different, too (see Table 3).

The valine derivative of dolastatin-10 (3) Compound **3** is the derivative of compound **1**, where dolavaline is replaced by the corresponding conventional amino acid valine. Four minima can be identified by the quenching procedure in vacuo, three of which are almost degenerate

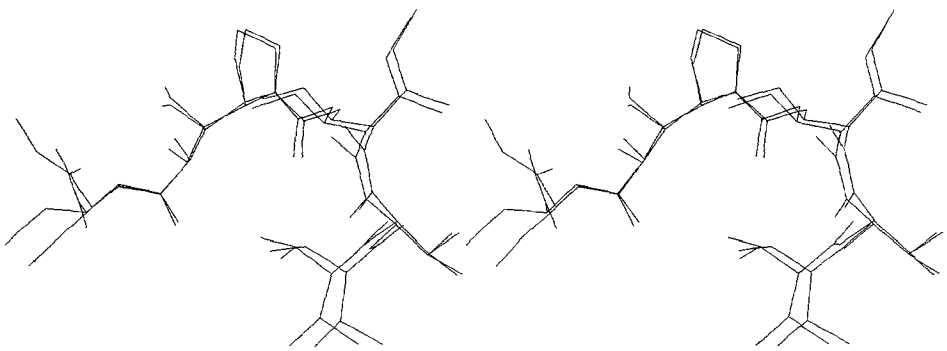

Fig. 6. Superposition of the two lowest energy conformers of compound **2h** in water. Hydrogens and water molecules are omitted for clarity.

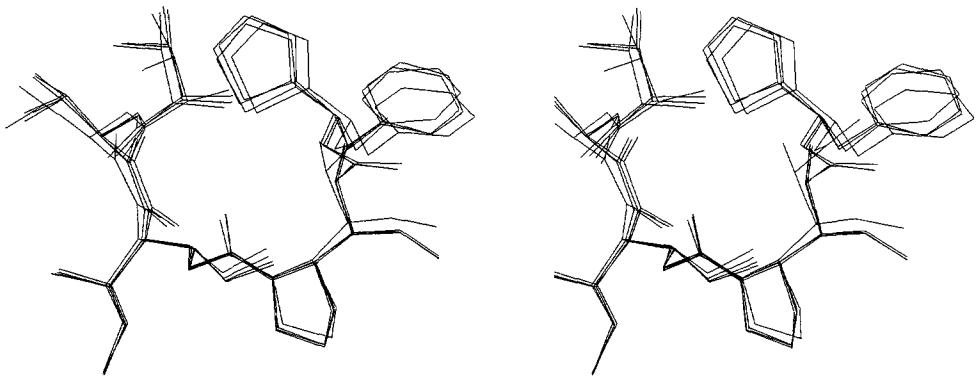

Fig. 7. Superposition of the four lowest energy conformers of compound **3** in water. Hydrogens and water molecules are omitted for clarity.

(see Table 4). The fourth minimum lies slightly higher in energy (≈ 1 kcal mol^{-1}) compared to the lowest minima. The conformational features of the lowest energy minima are quite similar. The global S-shape is always present, but the folding is still more pronounced with respect to the native peptide. This is due to the presence of an intramolecular hydrogen bond between the Val^1 nitrogen and the NH of dolaphenine, which acts as a donor. In addition, the hydrogens of the primary amino group point towards the thiazole ring, so that an interaction between these hydrogens and the π-electron system of the heterocycle can be hypothesised. As usual, Dap and Dil essentially maintain their conformation.

In water, the MD procedure allowed the identification of four conformers, lying within an energy range of 3.5 kcal mol^{-1} (see Table 4). These have all been found among the minimum-energy forms obtained from the first two MD runs (with initial temperatures of 300 and 400 K). Indeed, the simulation started at 500 K always produced conformers lying in a region of much higher energy, i.e., 20 kcal mol^{-1} above the most stable conformers.

The lowest minima have a quite similar shape, as can be seen from the superimposition shown in Fig. 7. The frequent presence of the intramolecular hydrogen bond between the Val^1 nitrogen and the Doe NH or between the Val^1 NH and the Dil carbonyl oxygen constrains the structure in a well-defined disposition, with an almost fixed and peculiar orientation of the Doe thiazole towards the N terminus. This orientation is favoured, too, by solvent–solute H-bonds, as discussed below. Compared to compound **1**, the differences in the 3D structure are strikingly evident (see Fig. 9); this is certainly a remarkable effect, considering the fact that **3** is derived from **1** by introducing a quite small structural variation. The valine derivative **3** has a 'cyclic' disposition, which directs the dolavaline residue in a quite different space region than that occupied by the same residue in **1**.

*The protonated valine derivative of dolastatin-10 (**3h**)*

Also in the case of the protonated species, the valine derivative proved to be the most flexible one among the compounds studied in the present work. Indeed, all conformers located by means of the quenching procedure lie in a quite narrow energy interval (1.3 kcal mol^{-1}), and five of the extracted frames converge to the same minima.

The torsional geometries of these five frames are listed in Table 4. All minima have, as a peculiarity, three intramolecular hydrogen bonds between the three ammonium protons and the Dil and Dap carbonyls and the Doe thiazole N. In spite of this, a certain variability is associated with some torsion angles, like τ_9, τ_{13} and τ_{14}. The values of the latter three angles govern the conformation

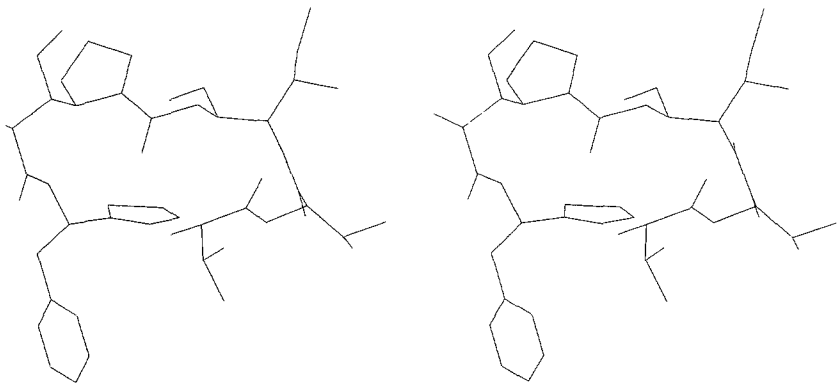

Fig. 8. Minimum-energy conformation of compound **3h** in water. Hydrogens and water molecules are omitted for clarity.

TABLE 4
TORSIONAL GEOMETRIES OF THE LOWEST ENERGY CONFORMERS OF **3** AND **3h** IN VACUO AND IN WATER[a]

Torsion angle	$\mathbf{3}_v$	$\mathbf{3}_w\mathbf{A}$	$\mathbf{3}_w\mathbf{B}$	$\mathbf{3}_w\mathbf{C}$	$\mathbf{3}_w\mathbf{D}$	$\mathbf{3h}_v\mathbf{A}$	$\mathbf{3h}_v\mathbf{B}$	$\mathbf{3h}_v\mathbf{C}$	$\mathbf{3h}_v\mathbf{D}$	$\mathbf{3h}_v\mathbf{E}$	$\mathbf{3h}_w$
τ_1	−51.2	−54.4	−54.5	−57.9	48.0	−88.0	−74.3	−98.7	−104.3	−78.0	−40.2
τ_2	178.5	−177.4	−178.1	−178.0	174.0	177.6	179.2	−178.7	178.6	−179.0	175.4
τ_3	−116.5	−120.5	−122.0	−115.4	−108.0	−113.2	−117.6	−113.3	−124.6	−116.1	−119.1
τ_4	86.9	86.3	85.2	97.9	88.7	98.0	100.6	97.9	99.3	97.1	87.0
τ_5	−5.8	−3.5	−4.6	−1.2	2.5	−11.1	−13.7	−7.7	−9.1	−12.2	−7.8
τ_6	−103.9	−105.6	−109.3	−109.3	−110.1	−105.8	−121.2	−110.2	−119.4	−110.3	−106.5
τ_7	168.0	164.3	162.4	164.0	165.0	162.0	150.8	158.1	163.0	152.2	151.0
τ_8	−158.8	−152.2	−151.1	−152.4	−148.7	−152.7	−99.8	−146.9	−71.9	−133.7	−155.9
τ_9	−87.6	−91.4	−89.2	−88.1	−91.4	−97.6	−179.2	−125.7	123.4	−161.0	−137.3
τ_{10}	175.4	177.2	170.7	171.2	177.6	177.9	174.2	−176.9	171.9	−175.6	176.3
τ_{11}	−89.7	−93.4	−89.9	−91.1	−90.3	−66.2	−77.2	−82.0	−80.7	−68.5	−81.1
τ_{12}	77.8	76.1	75.6	75.5	71.8	129.0	152.3	142.7	148.0	146.5	153.2
τ_{13}	−151.4	−146.5	−149.9	−149.3	−157.0	−140.6	−69.3	−80.9	−68.3	−74.3	−68.9
τ_{14}	116.1	123.7	131.2	132.9	91.6	−56.6	−79.2	−88.4	−74.9	−84.6	−65.7
τ_{15}	170.9	164.4	163.7	165.8	170.6	163.2	179.2	174.0	−179.2	−179.3	170.2
τ_{16}	82.8	83.3	84.8	77.4	122.6	140.6	135.1	124.6	139.6	134.6	90.1
τ_{17}	−171.4	−160.7	−157.8	−151.8	−165.5	−170.3	−169.1	−164.6	−169.5	−168.6	−166.5
τ_{18}	80.3	89.7	99.4	104.5	−78.6	74.8	63.4	−92.4	82.5	83.6	−87.60
ΔE	0	0	1.29	1.83	3.20	0	0.37	0.39	0.79	1.29	

[a] τ_i are torsion angles in degrees; see Fig. 2 for their definition. $\mathbf{3}_v$ represents the lowest energy conformer of **3** in vacuo; $\mathbf{3}_w\mathbf{A}$, $\mathbf{3}_w\mathbf{B}$, $\mathbf{3}_w\mathbf{C}$ and $\mathbf{3}_w\mathbf{D}$ are conformers of **3** in water, with increasing relative energy (ΔE, kcal mol^{-1}). $\mathbf{3h}_v\mathbf{A}$, $\mathbf{3h}_v\mathbf{B}$, $\mathbf{3h}_v\mathbf{C}$, $\mathbf{3h}_v\mathbf{D}$ and $\mathbf{3h}_v\mathbf{E}$ represent conformers of **3h** in vacuo, also with increasing relative energy. $\mathbf{3h}_w$ is the lowest energy conformer of **3** in water.

of the Dap residue and markedly distinguish the lowest energy minimum from the other low-energy conformers. The same angles and the more pronounced distortion from planarity of the peptide bond described by τ_5 are the most relevant differences with respect to the nonprotonated species.

In water, one low-energy conformer is obtained, while the next minimum lies at a 5 kcal mol^{-1} higher energy level. The torsional geometry of the lowest energy conformer is listed in Table 4, and its structure is depicted in Fig. 8. Of the three intramolecular H-bonds present in the base, only one seems to be sufficiently strong to survive in solvated surroundings, i.e., the one between an ammonium proton and the dolaisoleuine CO. As a consequence, τ_1 and τ_{16}, no longer constrained by the head–tail interaction between NH_3^+ and the thiazole N, have values quite different from those of the nonsolvated **3h**, but more similar to the nonprotonated form. The dolaproine residue retains a torsional geometry similar to that of the nonsolvated **3h**.

Interaction with the solvent

In the general formula of compounds **1**–**3**, several sites

Fig. 9. Superposition of the lowest energy conformers of compounds **1**, **2** and **3** in water. Hydrogens and water molecules are omitted for clarity.

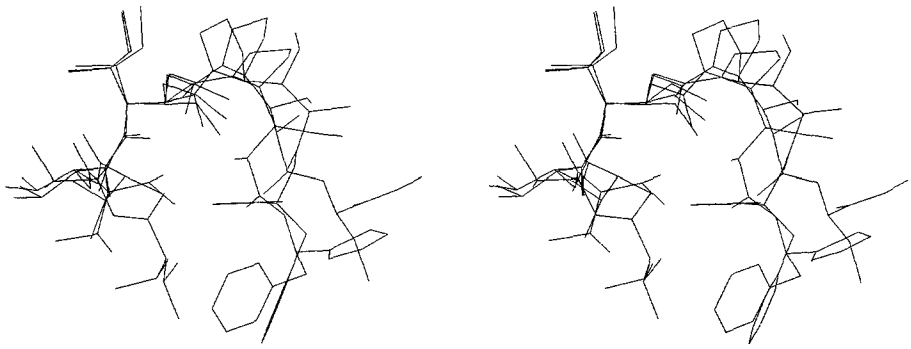

Fig. 10. Superposition of the lowest energy conformers of compounds **1h**, **2h** and **3h** in water. Hydrogens and water molecules are omitted for clarity.

can be identified which, in principle, could act as possible donors or acceptors of hydrogen bonds.

In compound **1**, the possible acceptors are the nitrogens in Dov, Dil and Dap, the thiazole N in Doe, and all oxygens, whereas the possible donors are the amide nitrogens in Val and Doe. However, the actual probability of forming hydrogen bonds with the solvent changes among the different moieties. The first evidence is the exclusive acceptor character of **1**. In fact, none of the conformers extracted from the trajectories shows the existence of hydrogen bonds between the Val and Doe NH and any water oxygen. On the other hand, the Val, Dil and Dap carbonyl oxygens, and the Dov N are always engaged in at least one hydrogen bond with the solvent. In the lowest energy minimum, the thiazole N acts as an acceptor as well.

The complete absence of intramolecular H-bonds may suggest that the folding of the structure is due to the hydrophobic components of the intramolecular potential and to the electrostatic attraction between the polar moieties of the molecule. For example, the empirical value for the charge on the dolaphenine thiazole sulphur is positive, whereas the dolavaline nitrogen is negatively charged. This may contribute to the head and tail portions of the peptide approaching each other.

The substitution of dolaphenine with cysteine in compound **2** adds two new potential hydrogen bond acceptors (the carboxylate oxygens). The carboxylate carbonyl oxygen indeed always forms at least one hydrogen bond with water. The Val, Dil and Dap carbonyl oxygens and the Dov nitrogen retain their pronounced acceptor capabilities. The Dov oxygen, which in the case of compound **1** did not show any tendency to form H-bonds, assumes an enhanced H-bond acceptor capability in the case of compound **2**.

The balance between moieties acting as acceptors or donors of H-bonds is slightly shifted in compound **3**, where the replacement of Dov with Val^1 introduces an additional donor moiety. The free NH, however, shows little tendency to interact with the solvent. Indeed, several conformers obtained by quenching points on the trajectory show an intramolecular hydrogen bond between Val^1 NH and the Dil carbonyl oxygen. One interesting situation was observed in the lowest energy minimum, where a water molecule is engaged in three hydrogen bonds with the solute; the two hydrogens interact with the dolaphenine carbonyl oxygen and the thiazole nitrogen, respectively. Simultaneously, the oxygen accepts an H-bond from a hydrogen of the Val^1 primary amino group. This stabilizes a quite complicated polycyclic conformation. The interaction of the dolaphenine thiazole nitrogen with water can be observed in two other minima among those with low energy.

In addition, the Val^1 N retains its acceptor capability, as shown by the presence of an H-bond Val^1 N-Doe NH in the low-energy conformers as well as in the minimum-energy conformer. The acceptor properties of the Val^1, Val^2, Dil and Dap carbonyl oxygens make them generally available for the interaction with water.

As far as the protonated species are concerned, of course the protonation adds a strong H-bond donor to the molecules studied. Indeed, the ammonium proton is involved in H-bonds with the solvent in the case of **1h**, while in **2h** it prefers to interact with the Dil carbonyl group. In the case of compound **3h**, the three ammonium protons interact with both the Dil carbonyl and two water molecules.

Like in compound **1**, all the carbonyl oxygens of **1h** are engaged in H-bonds with water. In addition, also the Dap OCH_3 oxygen acts as an acceptor in the lowest energy conformer. In the same conformers, two water molecules act as bridges between the Dap OCH_3 and the Doe NH, and between the Dil carbonyl and the ammonium proton.

In compound **2h**, the carbonyls are always engaged in H-bonds with the solvent, with the exception of the dola-isoleuine CO, which is involved in an intramolecular H-bond with the proton. The valine NH group acts as a donor in both minima. In conformer B also the cysteine NH acts as a donor.

Analogous considerations can be applied to compound **3h**. Also in this case, all carbonyls are engaged in H-bonds: the Dil CO with the ammonium protons and the

other with the solvent. The Val^2 and Doe NH groups both act as donors.

Conclusions

From a methodological point of view, two main observations are in order. First, we have shown that the CVFF potential in its standard form may give acceptable results when applied to the Dil, Dap and Doe residues and compared with ab initio data. As pointed out above, the reliability of the CVFF potential seems to be less satisfactory only in the case of Dov. A specific potential should be worked out in order to improve the capability of CVFF to reproduce structural features of the isolated amino acid Dov in a reliable way. This, however, is beyond the aims of the present study, especially considering that the modification of the internal structure of Dov could probably little affect the overall conformational behaviour of the dolastatin-10 derivatives.

The second observation concerns our computational procedure. The combination of MD simulations at increasing starting temperatures (a way of energizing the system) with a systematic sampling and geometry optimization of structures derived from the trajectory has been proved to be a reliable computational tool. This is shown by the fact that both in vacuo and in solution the procedure is potentially able to locate stable low-energy conformers; at the same time, it is useful also to indicate how large is the catching area of a given low-energy conformer. In fact we have shown that, when our molecular systems are considered as being isolated, most of the quenched structures converge towards a few well-defined conformers, regardless of the starting temperature.

This is a strong indication for the fact that these final forms are probably the most stable ones that can be obtained under these conditions. Furthermore, in the presence of water, the quenching of the MD trajectories initiated at the highest temperature (i.e., under conditions which probably allow to overcome relatively high potential barriers) did never produce minima that were more stable than those already identified along trajectories characterized by smaller initial contents of kinetic energy.

Regarding the molecular properties of compounds **1**–**3**, some concluding remarks follow.

One of the most evident features that can be noted by simply analyzing the sequence of dolastatin-10 (**1**) is its lipophilicity. The complete absence of free carboxylic functions and the presence of amino acids with branched hydrocarbon side chains give the peptide a prevailing hydrophobic character. As a consequence, most of the stable conformers found show a strongly folded conformation also in water. This is particularly true for the N-terminal portion of the molecule, which is, in addition, characterized by a pronounced rigidity. Possibly due to repulsive interactions among the bulky hydrophobic side chains, this part of the structure merely fluctuates by a few Ångstroms around the equilibrium position. These observations seem to agree with the description proposed for the peptide binding site at β-tubulin in the biological counterpart [10] as an apolar broad region with a certain rigidity. This region coincides with the putative binding site for the tripeptide A (Dov-Val-Dil-*O*-*t*-butyl) [12], the fragment arising from cleavage of the peptide bond Dil-Dap in **1**. This molecule retains a certain ability to inhibit tubulin polymerization, although not interfering with the GTP exchange.

The conformation of the same three N-terminal residues is not strongly affected by the mutations simulated in the present study, so that the mutated compounds could retain a certain similarity in interaction potentiality in this region as well. The alterations of the hydrophobic–hydrophilic balance within the native peptide result in significant modifications in the preferred conformations, which, however, are strictly localized in the region of the Dap and Doe residues. This is particularly evident in the case of compound **3**, where the valine demethylation gives rise to a completely altered conformational behaviour of the Dap and Doe residues only. When the protonated species are considered (see Fig. 10), it can be seen that the lowest energy conformers of **1h**, **2h** and **3h** show a rather good superposition of the N-terminal amino acids, in particular of Dil. In contrast with the nonprotonated compounds, also the Dap and Doe residues seem to possess a rather common spatial orientation. The presence of intramolecular H-bonds, which, in most low-energy conformers, involve the Dil carbonyl oxygen and the ammonium proton, suggests that the protonation gives rise to a certain reduction of the conformational freedom of dolastatin-10 and its derivatives.

In summary, the results obtained from a detailed sampling of the conformational space and the locations of the most stable forms have evidenced that the major factor in determining the conformational behaviour of compound **1** is the hydrophobicity of its residues, in spite of the presence of several polar groups. The MD experiments carried out on molecules that could be representative of a water-solvated system seem to suggest that the same basic structural features are present.

Even the apparently small simulated structural changes interfering with the hydrophobic–steric balance of the side chains dramatically alter this behaviour, thus completely modifying the location of the functions which are potentially able to interact with the biological partner. However, this mainly affects the C-terminal residues.

Acknowledgements

We wish to thank Prof. L. Villa for helpful discussions. Financial support from MURST and CNR (Rome) is gratefully acknowledged.

References

1 Gaius Plinius Secundus, Historia Naturalis, Libri IX and XXXII, ca. 60 A.D.

2 Pettit, G.R., Ode, R.H., Herald, C.L., Von Dreele, R.B. and Michel, C., J. Am. Chem. Soc., 98 (1976) 4677.

3 Pettit, G.R., Herald, C.L., Ode, R.H., Brown, P., Devens, J.G. and Michel, C., J. Nat. Prod., 43 (1980) 752.

4 Pettit, G.R., Kamano, Y., Herald, C.L., Fujii, Y., Kizu, H., Boyd, M.R., Boettner, F., Doubek, D.L., Schmidt, J.M. and Chapuis, J.-C., Tetrahedron, 41 (1993) 9151 and references cited therein.

5 Pettit, G.R., Kamano, Y., Herald, C.L., Tuinman, A.A., Kizu, H., Boettner, F., Schmidt, J.M., Baczynskyj, L., Tomer, K.B. and Bontems, R.J., J. Am. Chem. Soc., 109 (1987) 6883.

6 Pettit, G.R., Kamano, Y., Dufresne, C., Cerny, R.G., Herald, C.L. and Schmidt, J.M., J. Org. Chem., 54 (1989) 6005.

7 a. Pettit, G.R., Singh, S.B., Hogan, F., Lloyd-Williams, P., Herald, D.L., Burkett, D.D. and Clewlow, P.J., J. Am. Chem. Soc., 111 (1989) 5463.

For an ameliorated synthesis see:

b. Tomioka, K., Kanai, M. and Koga, K., Tetrahedron Lett., 32 (1991) 2395.

8 Pettit, G.R., Srirangam, J.K., Herald, D.L. and Hamel, E., J. Org. Chem., 59 (1994) 6127.

9 Pettit, G.R., Herald, D.L., Singh, S.B., Thornton, T.J. and Mullaney, J.T., J. Am. Chem. Soc., 113 (1991) 6692.

10 Bai, R., Pettit, G.R. and Hamel, E., J. Biol. Chem., 265 (1990) 17141.

11 Bai, R., Pettit, G.R. and Hamel, E., Biochem. Pharmacol., 39 (1990) 1941.

12 Bai, R., Pettit, G.R. and Hamel, E., Biochem. Pharmacol., 40 (1990) 1859.

13 Yamazaki, M., Tansho, S., Kisugi, J. and Muramoto, K., Chem. Pharm. Bull., 37 (1989) 2179.

14 Rich, D.H., Sun, E.T. and Boparai, A.S., J. Org. Chem., 43 (1978) 3624.

15 Biosym Technologies Inc., San Diego, CA.

16 Hehre, W.T., Radom, L., Schleyer, P. von R. and Pople, J., Ab Initio Molecular Orbital Theory, Wiley, New York, NY, 1986.

17 Fantucci, P., Mattioli, E., Marino, T. and Russo, N., In Russo, N., Anastassopoulou, J. and Barone, G. (Eds.) Properties and Chemistry of Biomolecular Systems, Kluwer, Dordrecht, 1994.